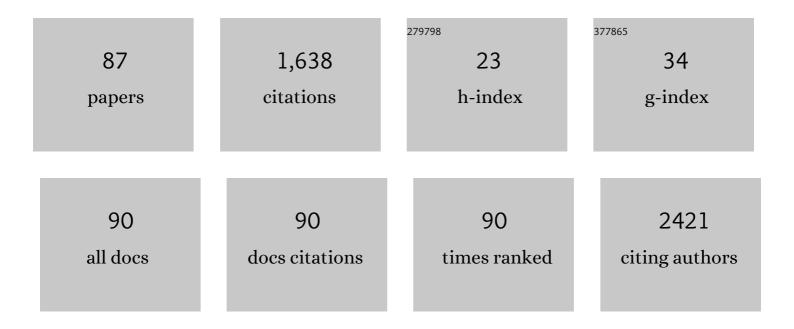
## **Chang Min Choi**

List of Publications by Year in descending order

Source: https://exaly.com/author-pdf/1297090/publications.pdf Version: 2024-02-01



#	Article	IF	CITATIONS
1	Role of additional PCBM layer between ZnO and photoactive layers in inverted bulk-heterojunction solar cells. Scientific Reports, 2014, 4, 4306.	3.3	83
2	Towards fabrication of high-performing organic photovoltaics: new donor-polymer, atomic layer deposited thin buffer layer and plasmonic effects. Energy and Environmental Science, 2012, 5, 9803.	30.8	78
3	Transparent and superhydrophobic films prepared with polydimethylsiloxane-coated silica nanoparticles. RSC Advances, 2013, 3, 12571.	3.6	66
4	Ultrathin TiO <sub>2</sub> Films on ZnO Electron-Collecting Layers of Inverted Organic Solar Cell. Journal of Physical Chemistry C, 2011, 115, 21517-21520.	3.1	65
5	Tandem ion mobility spectrometry coupled to laser excitation. Review of Scientific Instruments, 2015, 86, 094101.	1.3	58
6	CO oxidation catalyzed by NiO supported on mesoporous Al2O3 at room temperature. Chemical Engineering Journal, 2016, 283, 992-998.	12.7	51
7	Revealing the Synergy of Cation and Anion Vacancies on Improving Overall Water Splitting Kinetics. Advanced Functional Materials, 2021, 31, 2010718.	14.9	48
8	Conformational Dynamics in Ion Mobility Data. Analytical Chemistry, 2017, 89, 4230-4237.	6.5	46
9	Low Temperature CO oxidation over Iron Oxide Nanoparticles Decorating Internal Structures of a Mesoporous Alumina. Scientific Reports, 2017, 7, 40497.	3.3	38
10	Influence of surface roughness of aluminum-doped zinc oxide buffer layers on the performance of inverted organic solar cells. Applied Physics Letters, 2011, 98, .	3.3	37
11	Conformational changes in amyloid-beta (12–28) alloforms studied using action-FRET, IMS and molecular dynamics simulations. Chemical Science, 2015, 6, 5040-5047.	7.4	37
12	Oil–Water Separation Using Superhydrophobic PET Membranes Fabricated Via Simple Dipâ€Coating Of PDMS–SiO <sub>2</sub> Nanoparticles. Macromolecular Materials and Engineering, 2017, 302, 1700218.	3.6	37
13	Room temperature CO oxidation catalyzed by NiO particles on mesoporous SiO2 prepared via atomic layer deposition: Influence of pre-annealing temperature on catalytic activity. Journal of Molecular Catalysis A, 2016, 414, 87-93.	4.8	32
14	Emissive Nanoclusters Based on Subnanometerâ€6ized Au38 Cores for Boosting the Performance of Inverted Organic Photovoltaic Cells. Advanced Energy Materials, 2015, 5, 1500393.	19.5	31
15	Facile Mechanochemical Synthesis of Malleable Biomass-Derived Network Polyurethanes and Their Shape-Memory Applications. ACS Sustainable Chemistry and Engineering, 2021, 9, 6952-6961.	6.7	31
16	Quenching of photocatalytic activity and enhancement of photostability of ZnO particles by polydimethysiloxane coating. Journal of Materials Science, 2012, 47, 5190-5196.	3.7	28
17	Fabrication of conductive, transparent and superhydrophobic thin films consisting of multi-walled carbon nanotubes. RSC Advances, 2014, 4, 30368.	3.6	28
18	Structural Effect of Thioureas on the Detection of Chemical Warfare Agent Simulants. ACS Sensors, 2017. 2. 1146-1151.	7.8	27

#	Article	IF	CITATIONS
19	Superhydrophobic carbon fiber surfaces prepared by growth of carbon nanostructures and polydimethylsiloxane coating. Macromolecular Research, 2012, 20, 216-219.	2.4	25
20	Oxidation of Toluene on Bare and TiO <sub>2</sub> -Covered NiO-Ni(OH) <sub>2</sub> Nanoparticles. Journal of Physical Chemistry C, 2011, 115, 22954-22959.	3.1	24
21	TiO2/Ni Inverse-Catalysts Prepared by Atomic Layer Deposition (ALD). Catalysis Letters, 2011, 141, 854-859.	2.6	24
22	Fabrication of superhydrophobic thin films on various substrates using SiO <sub>2</sub> nanoparticles coated with polydimethylsiloxane: towards the development of shielding layers for gas sensors. RSC Advances, 2015, 5, 40595-40602.	3.6	24
23	CO Oxidation of Au–Pt Nanostructures: Enhancement of Catalytic Activity of Pt Nanoparticles by Au. Catalysis Letters, 2010, 134, 45-50.	2.6	23
24	Controlling the self-doping of epitaxial graphene on SiC via Ar ion treatment. Physical Review B, 2011, 84, .	3.2	23
25	Redox-buffer effect of Fe2+ ions on the selective olefin/paraffin separation and hydrogen tolerance of a Cu+-based mesoporous adsorbent. Journal of Materials Chemistry A, 2013, 1, 6653.	10.3	22
26	Organic Solar Cells Fabricated by One-Step Deposition of a Bulk Heterojunction Mixture and TiO <sub>2</sub> /NiO Hole-Collecting Agents. Journal of Physical Chemistry C, 2012, 116, 15348-15352.	3.1	21
27	Mesoporous SiO <sub>2</sub> Particles Combined with Fe Oxide Nanoparticles as a Regenerative Methylene Blue Adsorbent. ACS Omega, 2019, 4, 9745-9755.	3.5	21
28	Enhancement of Photocatalytic Activity of TiO2 by High-Energy Electron-Beam Treatment Under Atmospheric Pressure. Catalysis Letters, 2010, 135, 57-61.	2.6	20
29	Adsorption and Oxidative Desorption of Acetaldehyde over Mesoporous Fe <i><sub>x</sub></i> O <i><sub>y</sub></i> H <i><sub>z</sub></i> /Al <sub>2</sub> O <sub>3</sub> . ACS Omega, 2019, 4, 5382-5391.	3.5	20
30	Pentacene as protection layers of graphene on SiC surfaces. Applied Physics Letters, 2009, 95, 093107.	3.3	19
31	Adsorption and desorption of toluene on nanoporous TiO2/SiO2 prepared by atomic layer deposition (ALD): influence of TiO2 thin film thickness and humidity. Adsorption, 2013, 19, 1181-1187.	3.0	19
32	Gas-Phase Structural and Optical Properties of Homo- and Heterobimetallic Rhombic Dodecahedral Nanoclusters [Ag <sub>14–<i>n</i></sub> Cu <sub><i>n</i></sub> (C≡C <i>t</i> Bu) <sub>12</sub> X] <sup>+</sup> (X	= C <b>8).1</b> TjET(	Qq0090 O rgBT
33	2017, 121, 10719-10727. Peptide-Programmable Nanoparticle Superstructures with Tailored Electrocatalytic Activity. ACS Nano, 2018, 12, 6554-6562.	14.6	19
34	Photo-catalytic activity of hydrophilic-modified TiO 2 for the decomposition of methylene blue and phenol. Current Applied Physics, 2017, 17, 1557-1563.	2.4	18
35	Fe-oxide/Al2O3 for the enhanced activity of H2S decomposition under realistic conditions: Mechanistic studies by in-situ DRIFTS and XPS. Chemical Engineering Journal, 2022, 443, 136459.	12.7	18
36	Adsorption and Photocatalytic Decomposition of Toluene on TiO2 Surfaces. Catalysis Letters, 2010, 138, 76-81.	2.6	17

#	Article	IF	CITATIONS
37	Studies of degradation behaviors of poly (3â€hexylthiophene) layers by Xâ€ray photoelectron spectroscopy. Surface and Interface Analysis, 2014, 46, 544-549.	1.8	17
38	Charge, Color, and Conformation: Spectroscopy on Isomer-Selected Peptide Ions. Journal of Physical Chemistry B, 2016, 120, 709-714.	2.6	17
39	Engineering Interface on a 3D Co <sub><i>x</i></sub> Ni <sub>1–<i>x</i></sub> (OH) <sub>2</sub> @MoS <sub>2</sub> Hollow Heterostructure for Robust Electrocatalytic Hydrogen Evolution. ACS Applied Materials & Interfaces. 2022. 14. 9116-9125.	8.0	17
40	Temperature regulated-chemical vapor deposition for incorporating NiO nanoparticles into mesoporous media. Applied Surface Science, 2016, 385, 597-604.	6.1	16
41	Action-FRET of a Gaseous Protein. Journal of the American Society for Mass Spectrometry, 2017, 28, 38-49.	2.8	16
42	Excited States of Xanthene Analogues: Photofragmentation and Calculations by CC2 and Timeâ€Đependent Density Functional Theory. ChemPhysChem, 2016, 17, 3129-3138.	2.1	15
43	Surface Modification of TiO2 for Obtaining High Resistance against Poisoning during Photocatalytic Decomposition of Toluene. Catalysts, 2018, 8, 500.	3.5	15
44	Superhydrophobic Fabric Resistant to an Aqueous Surfactant Solution as Well as Pure Water for the Selective Removal of Spill Oil. ACS Applied Nano Materials, 2018, 1, 5158-5168.	5.0	15
45	Coreâ€Shell Structured Cobalt Sulfide/Cobalt Aluminum Hydroxide Nanosheet Arrays for Pseudocapacitor Application. Chemistry - an Asian Journal, 2019, 14, 446-453.	3.3	15
46	Organic photovoltaics with high stability sustained for 100 days without encapsulation fabricated using atomic layer deposition. Physica Status Solidi - Rapid Research Letters, 2012, 6, 196-198.	2.4	14
47	Ultrathin polydimethylsiloxane-coated carbonyl iron particles and their magnetorheological characteristics. Colloid and Polymer Science, 2012, 290, 1093-1098.	2.1	14
48	Reactivity and Stability of Ni Nanoparticles Supported by Mesoporous SiO2 and TiO2/SiO2 for CO2 Reforming of CH4. Catalysis Letters, 2014, 144, 56-61.	2.6	14
49	Initial Stage of Photoinduced Oxidation of Poly(3-hexylthiophene-2,5-diyl) Layers on ZnO under Dry and Humid Air. Journal of Physical Chemistry C, 2014, 118, 3483-3489.	3.1	14
50	Photocatalytic activity of Fe-loaded TiO2 particles towards NO oxidation: Influence of the intrinsic structures, operating conditions, and synergic effects of the surface hardening agent. Construction and Building Materials, 2021, 296, 123763.	7.2	14
51	Fabrication of superhydrophobic surfaces using structured colloids. Korean Journal of Chemical Engineering, 2013, 30, 1142-1152.	2.7	13
52	The structure of chromophore-grafted amyloid-β <sub>12–28</sub> dimers in the gas-phase: FRET-experiment guided modelling. Physical Chemistry Chemical Physics, 2016, 18, 9061-9069.	2.8	12
53	Superhydrophobic, flexible and gas-permeable membrane prepared by a simple one-step vapor deposition. Korean Journal of Chemical Engineering, 2016, 33, 1743-1748.	2.7	11
54	Reduction of NO by CO catalyzed by Fe-oxide/Al2O3: Strong catalyst-support interaction for enhanced catalytic activity. Applied Surface Science, 2020, 509, 145300.	6.1	11

#	Article	IF	CITATIONS
55	Unveiling a Three Phase Mixed Heterojunction via Phaseâ€Selective Anchoring of Polymer for Efficient Photocatalysis. Advanced Energy Materials, 2022, 12, .	19.5	11
56	Peptide-based bimetallic nanostructures with tailored surface compositions and their oxygen electroreduction activities. CrystEngComm, 2016, 18, 6024-6028.	2.6	10
57	Impact of humidity on the removal of volatile organic compounds over Fe loaded TiO2 under visible light irradiation: Insight into photocatalysis mechanism by operando DRIFTS. Materials Today Communications, 2021, 26, 102119.	1.9	10
58	Action-Self Quenching: Dimer-Induced Fluorescence Quenching of Chromophores as a Probe for Biomolecular Structure. Analytical Chemistry, 2017, 89, 4604-4610.	6.5	9
59	Comparative Studies of Mesoporous Fe2O3/Al2O3 and Fe2O3/SiO2 Fabricated by Temperature-Regulated Chemical Vapour Deposition as Catalysts for Acetaldehyde Oxidation. Catalysis Letters, 2018, 148, 454-464.	2.6	9
60	Enhanced removal efficiency of toluene over activated carbon under visible light. Journal of Hazardous Materials, 2021, 418, 126317.	12.4	9
61	Adsorbent/catalyst bi-functional Fe-ZSM-5 prepared by a simple CVD process for exhaust gas treatment. Applied Surface Science, 2022, 574, 151565.	6.1	9
62	Influence of electronâ€beam treatment of TiO <sub>2</sub> /Ti on properties of deposited Pt films. Surface and Interface Analysis, 2010, 42, 927-930.	1.8	8
63	Plasma-Assisted Non-Oxidative Conversion of Methane over Mo/HZSM-5 Catalyst in DBD Reactor. Topics in Catalysis, 2017, 60, 735-742.	2.8	8
64	Binding thiourea derivatives with dimethyl methylphosphonate for sensing nerve agents. RSC Advances, 2019, 9, 10693-10701.	3.6	8
65	Annealing Temperature-Dependent Effects of Fe-Loading on the Visible Light-Driven Photocatalytic Activity of Rutile TiO2 Nanoparticles and Their Applicability for Air Purification. Catalysts, 2020, 10, 739.	3.5	8
66	Visible-Light-Induced Oxidation of Poly(3-hexylthiophene-2,5-diyl) Thin Films on ZnO Surfaces under Humid Conditions: Study of Light Wavelength Dependence. Journal of Physical Chemistry C, 2016, 120, 19942-19950.	3.1	7
67	Unveiling the Complexity of the Degradation Mechanism of Semiconducting Organic Polymers: Visible-Light-Induced Oxidation of P3HT Films on ZnO/ITO under Atmospheric Conditions. Journal of Physical Chemistry C, 2017, 121, 18692-18701.	3.1	6
68	Secondary ion mass spectrometry (SIMS) with Bi3+ primary ions as a sensitive probe of surface structures of heterogeneous catalysts. International Journal of Mass Spectrometry, 2018, 433, 47-54.	1.5	6
69	Ion mobility resolved photoâ€fragmentation to discriminate protomers. Rapid Communications in Mass Spectrometry, 2019, 33, 28-34.	1.5	6
70	Preparation of ZnO/Al2O3 catalysts by using atomic layer deposition for plasma-assisted non-oxidative methane coupling. Journal of the Korean Physical Society, 2016, 68, 1221-1227.	0.7	5
71	Photo-induced linkage isomerization in the gas phase probed by tandem ion mobility and laser spectroscopy. Physical Chemistry Chemical Physics, 2018, 20, 12223-12228.	2.8	5
72	Dynamic secondary ion mass spectroscopy of Au nanoparticles on Si wafer using Bi3+ as primary ion coupled with surface etching by Ar cluster ion beam: The effect of etching conditions on surface structure. Journal of Applied Physics, 2018, 123, 015303.	2.5	5

#	Article	IF	CITATIONS
73	TOF-SIMS Analysis Using Bi <sub>3</sub> <sup>+</sup> as Primary Ions on Au Nanoparticles Supported by SiO <sub>2</sub> /Si: Providing Insight into Metal–Support Interactions. ACS Omega, 2019, 4, 13100-13105.	3.5	5
74	Positive Effects of Impregnation of Fe-oxide in Mesoporous Al-Oxides on the Decontamination of Dimethyl Methylphosphonate. Catalysts, 2019, 9, 898.	3.5	5
75	The nano-fractal structured tungsten oxides films with high thermal stability prepared by the deposition of size-selected W clusters. Applied Physics A: Materials Science and Processing, 2017, 123, 1.	2.3	5
76	Surface Structures of Fe–TiO <sub>2</sub> Photocatalysts for NO Oxidation. ACS Applied Materials & Interfaces, 2022, 14, 24028-24038.	8.0	5
77	Synthesis of ZnO nanoparticles by spray-pyrolysis method and their photocatalytic effect. , 2010, , .		4
78	Porous Silica Particles as Oil Absorbents: Comparison of Mesoâ€, Macroâ€, and Meso/Macroâ€Structures. Bulletin of the Korean Chemical Society, 2015, 36, 1751-1757.	1.9	4
79	Oxidized Ni Nanostructures Supported by Mesoporous <scp>Al<sub>2</sub>O<sub>3</sub></scp> : Relationship between the Structure and Reactivity for <scp>CO</scp> Oxidation Studied via Photoemission Spectroscopy. Bulletin of the Korean Chemical Society, 2016, 37, 674-679.	1.9	4
80	Atomic Layer Deposition for Preparation of Highly Efficient Catalysts for Dry Reforming of Methane. Catalysts, 2019, 9, 266.	3.5	4
81	Kinetic study of azobenzene <i>E</i> / <i>Z</i> isomerization using ion mobility-mass spectrometry and liquid chromatography-UV detection. Analyst, The, 2020, 145, 4012-4020.	3.5	4
82	Surface Modulation of 3D Porous CoNiP Nanoarrays In Situ Grown on Nickel Foams for Robust Overall Water Splitting. International Journal of Molecular Sciences, 2022, 23, 5290.	4.1	2
83	Study on the changes of surface property of grown C-TiO <inf>2</inf> films by O <inf>2</inf> plasma treatment. , 2010, , .		0
84	Changes in the surface structure of Pd/Ta <sub>2</sub> O <sub>5</sub> by oxygen and CO studied using Xâ€ray Photoelectron Spectroscopy (XPS). Surface and Interface Analysis, 2011, 43, 1371-1376.	1.8	0
85	Excited States of Xanthene Analogues: Photofragmentation and Calculations by CC2 and Time-Dependent Density Functional Theory. ChemPhysChem, 2016, 17, 2951-2951.	2.1	0
86	Extreme size dependence of the oxidation behavior of molybdenum clusters. AIP Conference Proceedings, 2018, , .	0.4	0
87	Ga-ion beam surface modification of glass using a custom-built liquid metal ion beam. Journal of Applied Physics, 2022, 131, 014901.	2.5	Ο